*J. Fluid Mech.* (1972), *vol.* 54, *part* 4, *pp.* 599–611
*Printed in Great Britain*



# Convection in boxes: experiments

By K. STORK AND U. MÜLLER
Lehrstuhl für Strömungslehre, Universität Karlsruhe

(Received 11 February 1972)

Convective motions in rectangular boxes with one side horizontal have been studied. The critical Rayleigh numbers were determined. In most cases cell patterns with rolls parallel to the shorter side wall of the rectangular box were observed. The results have been compared with the known theoretical results of Davis (1967). In general, good agreement has been found.

## 1. Introduction

The influence of lateral walls on the onset of convection in horizontal fluid layers heated from below has been repeatedly subjected to theoretical investigation in recent years. Pellew & Southwell (1940) and Zierep (1963) have already pointed out the dependence of the critical Rayleigh number on the lateral boundaries in heated fluids. By simplifying the boundary conditions on the lateral walls, i.e. by assuming slip flow, Zierep (1963) first calculated the influence of the walls. Davis (1967) gave a detailed theoretical investigation of the relevant linear stability problem for convection in boxes of rectangular shape. In order to gain reliable results, even for boxes of small aspect ratio, all boundaries were considered to be rigid and perfect heat conductors, i.e. the disturbances in velocity and temperature caused by convection are assumed to vanish at the walls. The latter assumption ensures that the temperature distribution in the lateral walls remains linear in the vertical direction even after the onset of convection. Such boundary conditions, however, exclude a presentation of the solution in analytical form as such a solution is usually obtained by separation of variables. Davis applied a Galerkin method to the linearized equations of convection. It is known that Galerkin's method is an approximation method and consequently yields only approximate critical Rayleigh numbers (upper bounds) and eigenfunctions. The trial functions used in Davis' calculations are confined to forms approximating convection rolls with only two velocity components dependent on three space variables. However, Davis has shown that more general convection patterns such as polygonal cells can be described by superposing finite convection rolls of perpendicular direction. It turns out in the case of lateral side walls that convection-roll systems with the minimum critical Rayleigh number are selected out of such superpositions. Only if the critical Rayleigh numbers of the two different roll systems are equal or nearly equal will more sophisticated selection processes (such as disturbances of finite amplitude or variations of properties) become dominant (see Segel 1969).

Although the results of Davis (1967) were extended in further articles by

Segel (1969) and Davies-Jones (1971) and were recalculated by Catton (1970), they still represent the basic theoretical results for convective flow in rectangular boxes. Therefore we quote them here.

'The results obtained for boxes with a width-to-depth ratio $h/d$ in the range $\frac{1}{4} \leqslant h/d \leqslant 6$ are the following.

(i) The preferred mode is always some number of finite rolls (two non-zero velocity components dependent on three spatial variables) with axes parallel to the short side (square boxes excepted).

(ii) When the depth is the smallest dimension, finite rolls of near-square cross-section are predicted. Otherwise narrower finite rolls appear.

(iii) The critical Rayleigh number decreases rapidly to the value 1708 as the horizontal dimensions increase so that most experiments, which use thin layers, would appear to have onset occur at about $Ra_c = 1708$.'

To the authors' knowledge, no detailed experimental investigation of convective flow in rectangular vessels heated from below has yet been performed. The experiments reported here are aimed at verifying the theoretical results known so far. As the experiments described comply largely with the assumptions of Davis (1967) the results are especially suitable for comparison with his results. Therefore, throughout this paper, we have adopted his notation which is as follows. If rectangular boxes are fixed in a rectangular co-ordinate system in such a way that the axes coincide with three edges, then convection rolls parallel to the $y$ axis are termed finite $x$-rolls and those parallel to the $x$ axis finite $y$-rolls.

## 2. Experimental set up and technique

A standard constant-temperature plate apparatus like that used by Koschmieder (1966) was employed for the experiments. A schematic diagram of this is given in figure 1. The apparatus is axisymmetric about its vertical axis. The fluid (*a*) was enclosed between a 10 mm thick copper disk (*b*) of 200 mm diameter and a 3 mm thick glass disk (*c*). The distance between the plates was 10 mm for all experiments. Both plates could be maintained at a constant temperature by circulating fluid from controlled baths below or above the plates respectively. Cooling or heating fluid was fed into the system at several points, uniformly distributed on the circumference, to ensure as uniform a temperature distribution as possible. The apparatus was designed such that the fluid was easily accessible by separating the upper container (*d*) together with the glass plate from the lower section (*e*). The glass and copper plates were maintained parallel and at the fixed distance of 10 mm by three spacers of equal size. Rectangular frames of different sizes were located in the test volume. These frames were designed so that two walls could be shifted parallel to each other while the others were held at definite distances. Convection was investigated in the rectangular volume formed by the frame and the upper and lower plates. Four ferro–constantan thermocouples of 0·5 mm diameter were used to determine two temperature differences between the upper and lower boundaries of the fluid layer. The thermocouples were attached to the plates near the side walls. The potential difference was measured by a digital voltmeter ($1\,\mu\text{V} \simeq 1{\cdot}9 \times 10^{-2}\,^{\circ}\text{C}$)

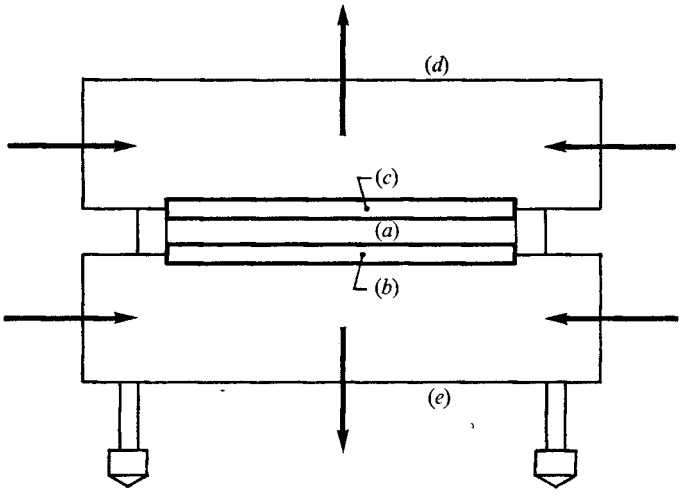


FIGURE 1. Schematic section of the apparatus.

and simultaneously recorded on a chart recorder during the long runs. Bayer silicon oil M300 was used as a test fluid, aluminium powder being added as a tracer. The silicon oil had the following properties:

$$\rho = 0{\cdot}994 - 8{\cdot}97 \times 10^{-4} t \,(\mathrm{g\,cm^{-3}}),$$
$$\nu = 590 \exp(-0{\cdot}017t)\,(\mathrm{cm^2\,s^{-1}}),$$
$$\lambda = 0{\cdot}1416 - 10^{-4} t \,(\mathrm{kcal\,m^{-1}\,h^{-1}\,grad^{-1}}),$$
$$\beta = 8{\cdot}97 \times 10^{-4}\,(\mathrm{grad^{-1}}),$$
$$c = 0{\cdot}36\,(\mathrm{kcal\,kg^{-1}\,grad^{-1}}),$$

where $\rho$ is the density, $\nu$ the kinematic viscosity, $\lambda$ the thermal conductivity, $\beta$ the coefficient of thermal expansion and $c$ the specific heat. Because the measurements were taken for a relatively large range of temperature differences the variation of $\rho$, $\nu$ and $\lambda$ with temperature had to be considered; in the above relations $t$ is the temperature in degrees Celsius.

For the determination of the critical temperature difference between upper and lower plates two independent methods were applied. The first is based on the visualization of the convection pattern with aluminium particles. At first particles which were at first randomly orientated moved in preferred directions even under very low shear flow. On a dark background (the copper plate was covered with black paint†) visible light and dark contrasts developed soon after convection started. If any such regularities were observed the temperature differences between top and bottom were registered. As the heating of the fluid was for long periods (1–3 h, quasi-static heating) the critical temperature could be estimated with reasonable accuracy. This method has proved to be very reliable. The second method uses the time history of the temperature difference on an automatic recorder. The start of convection can be noticed in this case by

† The paint film was very thin so that the uniform temperature distribution was not disturbed.

a kink in the temperature–time plot. Generally the convection started near the central area of the test volume, as the heating process was slightly unsteady, and the effect of the frictional resistance at the side walls was smallest in the centre. Since the thermocouples were fixed near the side walls, to keep the wiring influences as small as possible, they registered the start of convection later than could be observed optically. The second method therefore gave critical Rayleigh numbers which were, on the average, 5 % above those gained by optical observation. All values plotted in this article were determined by the first method. Recording the temperature difference was used only for cross checking.

Using the above described apparatus and techniques, the following test series were performed. For constant ratios of the height $d$ to $h_1$, the length of one side wall ($h_1/d = 6, 5, 4, 3, 2$) the length $h_2$ of the other side wall was varied from $0{\cdot}5d$ to $6d$ in small increments of $0{\cdot}2d$.† For the above frames, as well as all square frames, the critical Rayleigh number, the number of cells and the cell shape were determined.

## 3. Some comments on thermal boundary and initial conditions

Davis assumes in his linear theory that all surrounding walls of the test volume are perfect heat conductors. Such conditions cannot be realized in experiments employing visualization techniques because transparent materials are generally poor heat conductors. In our experiments crystal glass, the best transparent heat conductor available, was chosen as the upper plate. If a good heat conductor like copper is taken as the material for the side walls then horizontal temperature gradients form in the glass where the copper and glass join. These cause higher temperatures in the copper walls than in the adjacent liquid and, therefore, undesirable convection flow near the heated vertical planes occurs. The above effect was observed to occur at Rayleigh numbers far below the expected critical one for uniform boundary conditions. In this case only one convection roll developed along the side walls. This obvious difficulty was overcome in the following way. For the side walls a material was chosen whose thermal conductivity was as near as possible to the heat conductivity of the fluid. A suitable material is a P.V.C. product from BASF with a heat conductivity of

$$0{\cdot}126\,\mathrm{kcal\,m^{-1}\,h^{-1}\,grad^{-1}}$$

(for $0 \leqslant t \leqslant 60\,^{\circ}\mathrm{C}$) (compared with a $\lambda = 0{\cdot}140\,\mathrm{kcal\,m^{-1}\,h^{-1}\,grad^{-1}}$ for $t \approx 20\,^{\circ}\mathrm{C}$ of the silicon oil). This combination of materials prevents an uneven heating of the fluid and the side walls, and an essentially linear vertical temperature distribution is maintained if the thermoconvection is of small amplitude. This condition holds at the critical point, which is essentially the condition of interest. It may be expected that the temperature disturbance at the side walls is negligible. However, we should be aware of the partly insulating character of the side walls due to the relatively poor heat conductivity of P.V.C. Hence we are in fact dealing with mixed boundary conditions as far as temperature and heat conduction are concerned, though the insulating effect is not as important.

† For simplicity we shall henceforth refer to the width-to-depth ratios as $h_1$ and $h_2$.

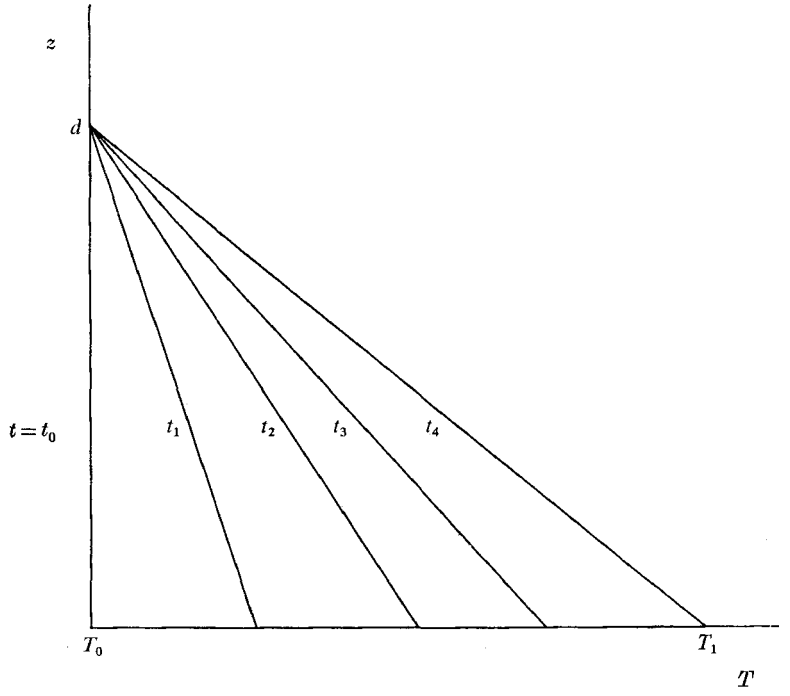


FIGURE 2. Temperature profiles caused by slowly increasing the temperature at the lower side of the layer.

As with many other investigations on cellular convection the article of Davis refers to the marginal stability case. The question of how this state is finally reached is not dealt with. Every experimental investigation, however, is faced with the problem of achieving this steady state, since the mode initiating this condition might be important, with the final steady state dependent on the initial conditions. In our case these initial conditions are provided basically by the heating process. Because it was intended here to investigate the influence of the lateral walls, the heating process was performed slowly to ensure that the influence of the walls dominates the disturbances caused by the unsteady heating and conduction processes. Longer heating times are required when the ratio of the side-wall length to the depth of the layer is increased. If an initial critical temperature difference is assumed, a simple calculation gives rise times of about 7 min for the development of a linear temperature profile (see Carslaw & Jaeger 1959, for instance). Of course, the heating time has to be much greater if the heating is to be quasi-steady and the temperature profile (see figure 2) is to be linear at all times. In the experiments described here the heating times varied between 1 and 3 h. However, when the distances between the side walls were comparatively large, polygonal cells formed in the centre of the test volume in spite of the long heating times. These convection cells, once formed, were so stable that even supercritical heating could not alter their shape. The question arose at this point of whether a change in the initial conditions could generate convection flows of roll shape as predicted by Davis. Therefore the initial

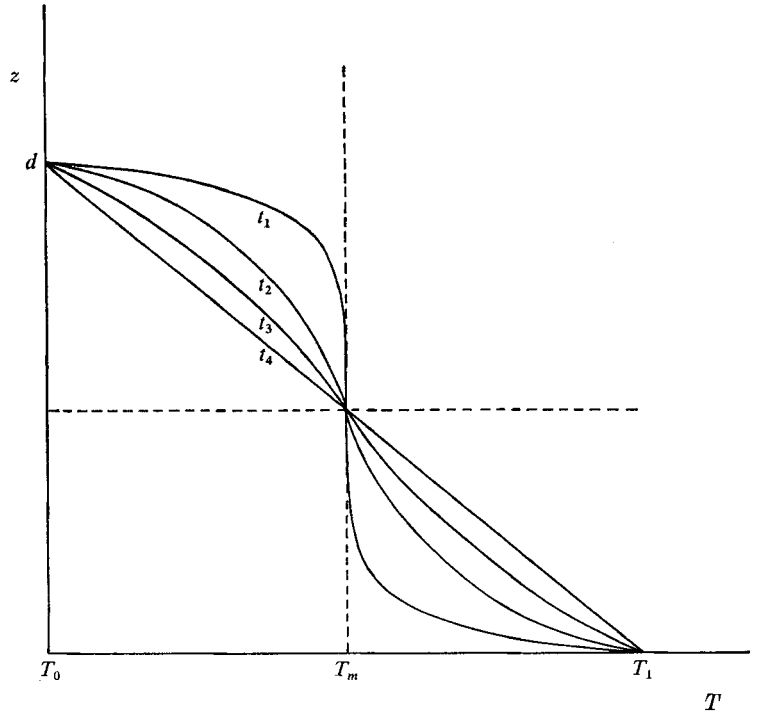


FIGURE 3. Temperature profiles caused by slowly increasing the temperature at the lower side and lowering it at the upper side of the layer.

conditions were changed in the following way. First, the critical state (onset of convection) was established by slow heating. At this stage the upper part ($d$) of the apparatus (cooling section, see figure 1) was removed. The fluid was then brought to a uniform temperature $T_m$ by careful stirring. After this procedure the upper and lower parts were fixed together again. During the whole procedure the temperatures of the heating and cooling fluid in the lower and upper systems were kept constant. The steady state of linear temperature distribution was then reached by a compensation process as sketched in figure 3. After a few minutes, in most cases, a pattern of convection rolls was observed and was stable even under supercritical heating conditions. Systems of different convection patterns appeared if the frames were of square or nearly square shape.

## 4. Evaluation of the measurements and error analysis

The critical Rayleigh number was calculated according to the relation

$$Ra_c = g\beta\Delta T_c d^3 c\rho/\lambda\nu,$$

where $g$ is the acceleration of gravity, $\beta$ is the coefficient of thermal expansion of the liquid, $\Delta T_c$ is the critical temperature difference between upper and lower plate, $d$ is the layer thickness, $\lambda$ the thermal conductivity, $\nu$ the kinematic viscosity, $c$ the specific heat and $\rho$ the density. The quantities $\rho$, $\lambda$ and $\nu$ are

generally dependent on the local temperature. The values at an average temperature $T = \frac{1}{2}(T_b + T_c)$† were then used to evaluate the Rayleigh number.

The crucial point in the present investigation was the measurement of the critical temperature difference. This measurement contains two basic sources of errors. Random errors due to inaccuracies in calibrating the thermocouples and reading the digital voltmeter, and inaccuracies in the thermocouples and the associated circuitry amounted to about 2 % of the total critical temperature difference. A systematic error of at most 5 % of $\Delta T_c$ is attributed to the optical method by which the onset of convection was determined. (A 5 % difference in $\Delta T_c$ occurred on the average when an optical observation rather than the chart recorder was used for measuring $\Delta T_c$.)

Another systematic error of at most 0·5 % was caused by the fact that the thermocouples were attached to the surface of the upper and lower plate rather than being contained in the plates. Next in importance for the accuracy in the measurement of the temperature is the maintenance of a definite layer thickness, because the Rayleigh number depends on the third power of the layer thickness. The error was less than 1 % owing to the spacers being of guaranteed length $d = 10 \pm 0{\cdot}01$ mm. The uncertainties in the values used for the material properties were presumably of the following orders: for viscosity $\Delta\nu/\nu \approx 0{\cdot}5$ %, for specific heat $\Delta c/c \approx 1$ %, for density $\Delta\rho/\rho \approx 0{\cdot}5$ % and for the coefficient of thermal expansion $\Delta\beta/\beta \approx 2$ %. Thus this error analysis shows that the critical Rayleigh number may contain estimable random errors up to a maximum of 7 %. However, the different errors will in general at least partly compensate each other, so that actually the experimental error is less. The systematic error in the temperature measurement of 5 % must be considered as an upper limit as the optical method gives critical temperature differences which are possibly too low while, on the other hand, the chart recorder gives values which are too high.

## 5. Results and discussions

### 5.1. *The critical Rayleigh numbers*

The quantitative results of the present investigation can be seen in figures 4 (*a*)–(*e*). The critical Rayleigh numbers $Ra_c$ are plotted versus the width-to-depth ratio $h_2$, with $h_1$ fixed. From these figures it can be stated that for small $h_2$ the critical Rayleigh numbers show a sharp drop with increasing values of $h_2$, i.e. with increasing horizontal dimension of the box. In all cases considered the Rayleigh numbers reach at an $h_2$ of about 2 a nearly constant value of about 2000, which is fairly near to the value of 1708 for thin liquid layers not confined by side walls. For comparison the theoretical results of Davis and some values from Catton's (1970) calculations are recorded. It is clear from the figures that the experimental values are generally below the theoretical ones. The following more detailed trends can be noticed.

Within one series of tests ($h_1$ = constant) the discrepancies between theoretical and experimental results increase as the box becomes narrower (small $h_2$).

† $T_c$ = temperature at the upper plate; $T_b$ = temperature at the lower plate.

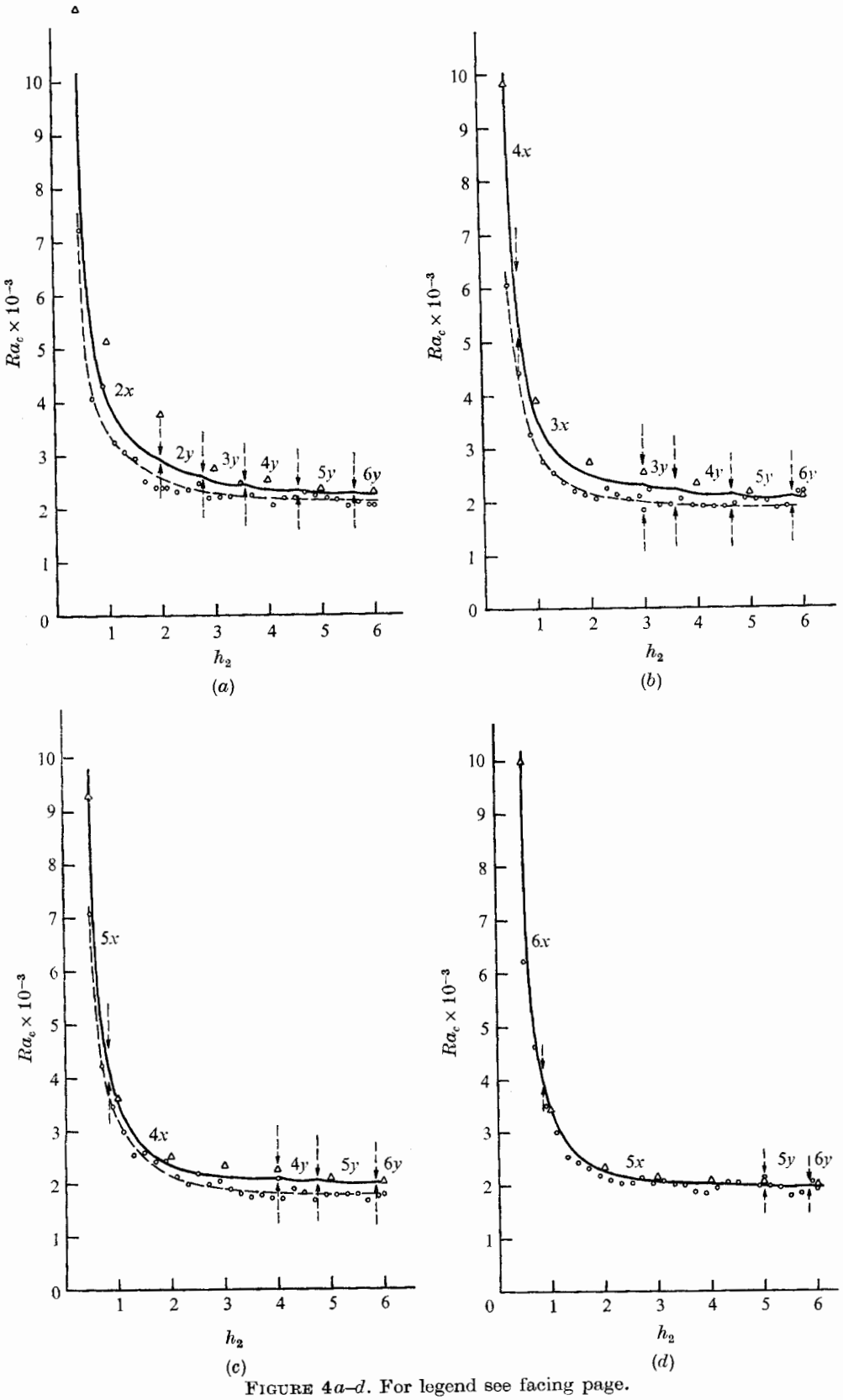


FIGURE 4*a–d*. For legend see facing page.

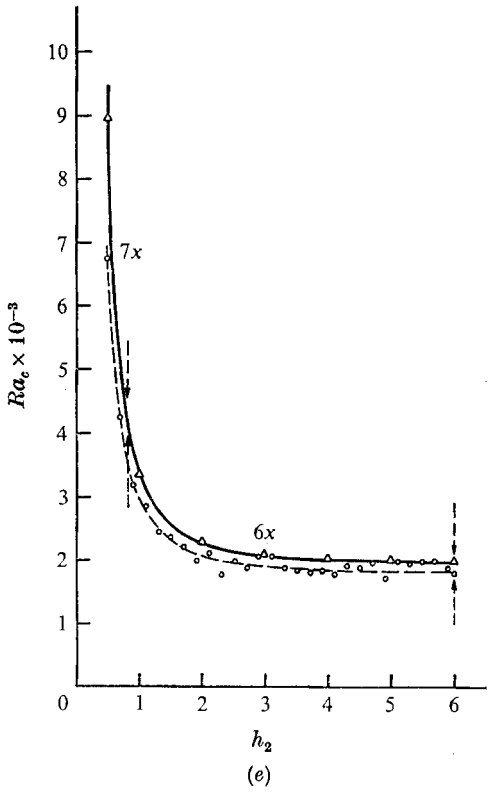


FIGURE 4. Critical Rayleigh number $Ra_c$ versus $h_2$. Theory: ——, Davis; △, Catton. ○, experimental results. (*a*) $h_1 = 2$. (*b*) $h_1 = 3$. (*c*) $h_1 = 4$. (*d*) $h_1 = 5$. (*e*) $h_1 = 6$.

Especially for $h_2 < 1$ the differences may become as large as one third of the calculated Rayleigh numbers. An additional decrease in $h_1$ enlarges the differences. There are indications that test series for which the ratio $h_1$ is odd exhibit for $h_2 < h_1$ greater discrepancies than those for which $h_1$ is even (compare, for instance, figure 4(*a*) with figure 4(*b*), or figure 4(*b*) with figure 4(*c*)). The last statement reflects the observed phenomenon that the development of an even number of convection rolls is preferred to the formation of an odd number. This phenomenon will be discussed later. The discrepancies between the experimental and the theoretical curves are partly caused by the fact that a Galerkin method (or Ritz method) gives only upper bounds when $Ra_c$ is calculated using this method. Further on in his article Davies-Jones (1971) proves that finite rolls aligned perpendicular to one side wall, as was assumed by Davis, are not exact solutions of the linearized convection problem. Using roll-like trial functions he gains a satisfactory approximation to the true solution, but the approximate values are always above the exact solution. These statements essentially explain the discrepancies in the graphs for ratio $h_2$ greater than about 1·5 if in addition the error analysis of § 4 is considered. The large discrepancies (up to 30 %) in the region of steep slope of the curves in figures 4(*a*)–(*e*) ($h_2 < 1{\cdot}5$) have a different cause. The insufficient observance of the thermal boundary condition (partly

insulating side walls) influences the results increasingly if the distance between the side walls decreases. Calculations of Davies-Jones (1971) show that, in the case of insulated side walls, the Rayleigh numbers are below those in the case of conducting side walls. The difference is considerable in the range $h_2 < 1{\cdot}5$ (for instance, for $h_2 = 1$ $\Delta Ra_c/Ra_c \approx 40\,\%$). The discrepancies between theory and experiment in this range are therefore evident.

It is, however, of interest to state that disturbances of finite amplitude cannot contribute to the discrepancies between theory and experiment. As Joseph (1965) has proved, the critical Rayleigh numbers cannot be lowered by increasing the disturbance amplitude. It is clear that during the heating process temperature disturbances of finite amplitude are present.

The kinks in the curves calculated by Davis (1967) (solid lines in figures 4 (*a*)–(*e*)) and caused by convection arrangements of different numbers of rolls could not be exhibited by these experiments since this characteristic of the curves is on a scale within the margin of error.

### 5.2. *Shape and number of cells*

Figures 5–7 (plates 1–3) show convection cells in the final steady state near to the critical conditions. The two most typical formation processes of convection patterns are presented in figures 8 and 9 (plate 4). From figure 8 it can be seen that the convection starts by forming annular type or strongly bent rolls. Such phenomena were observed in all experiments except in cases of very small rectangular boxes ($h_2 < 1$). With increasing time the circular convection cells decay and the remaining parts orient themselves more and more to be parallel to the shorter side wall, forming patterns as predicted by Davis. The rolls nearest to the side walls, however, remain bent under the influence of the corners.

Completely different from this type of development is the formation of cell patterns in figure 9. Almost at the beginning of the convection the final symmetric pattern appears, and becomes more pronounced with increasing time. These symmetric cell systems proved to be very stable even if the heating was continued to highly supercritical conditions. Only by changing the heating process itself, i.e. changing the initial conditions as was described in § 3, could convection patterns according to Davis's theory, in some cases, be generated. In the following we shall discuss the different test series in more detail.

*Test series* 1 ($h_1 = 2$). In all experiments finite rolls appear and are parallel to the shorter side walls. The arrangement of cells in the case of a square frame can be interpreted as an indifferent combination of both $x$- and $y$-rolls (see figure 5). On considering the numbers of rolls in 5 of a total of 30 performed experiments, a difference of one cell was found. This can be seen from figure 10, where all experiments are listed in a $h_1$–$h_2$ plot and the areas of different cell numbers are separated by lines predicted by theory. The phenomenon can easily be explained. In the marginal area between two different numbers of cells the critical Rayleigh numbers are so close together that both states can be reached only if the disturbances are intensive enough at the onset of convection. As the theory predicts, one of these states is less stable, but the experiments show that if once established both configurations are of considerable stability and even supercritical heating

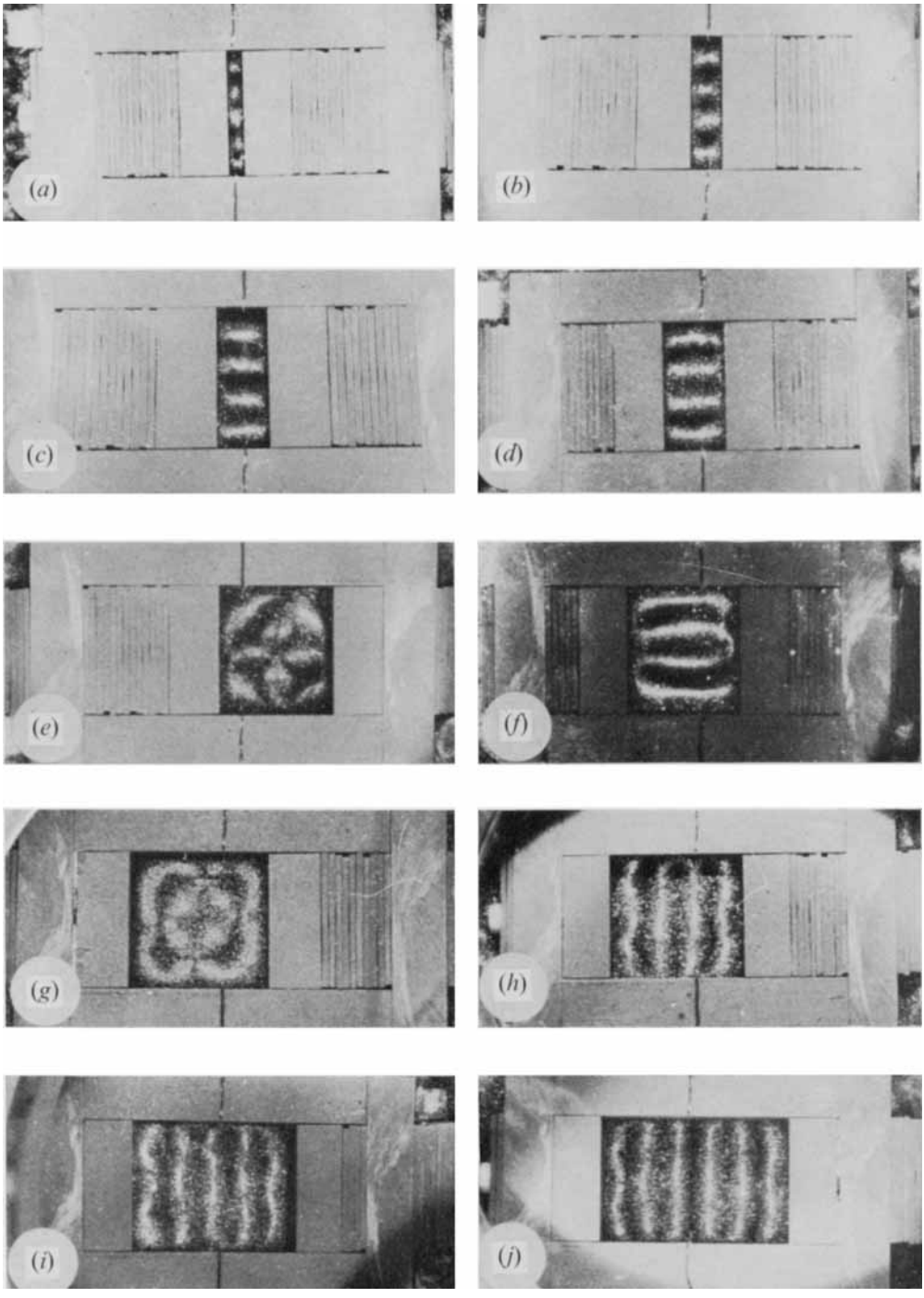


FIGURE 5. Convection cells in rectangular boxes with $h_1 = 2{\cdot}0$. (*a*) $h_2 = 0{\cdot}5$, 2 finite $x$-rolls. (*b*) $h_2 = 1{\cdot}1$, 2 finite $x$-rolls. (*c*) $h_2 = 2{\cdot}0$, combination of $x$- and $y$-rolls. (*d*) $h_2 = 2{\cdot}9$, 3 finite $y$-rolls. (*e*) $h_2 = 3{\cdot}9$, 4 finite $y$-rolls. (*f*) $h_2 = 4{\cdot}5$, 4 finite $y$-rolls. (*g*) $h_2 = 4{\cdot}7$, 4 finite $y$-rolls. (*h*) $h_2 = 5{\cdot}1$, 5 finite $y$-rolls, (*i*) $h_2 = 5{\cdot}7$, 6 finite $y$-rolls. (*j*) $h_2 = 6{\cdot}0$, 6 finite $y$-rolls.

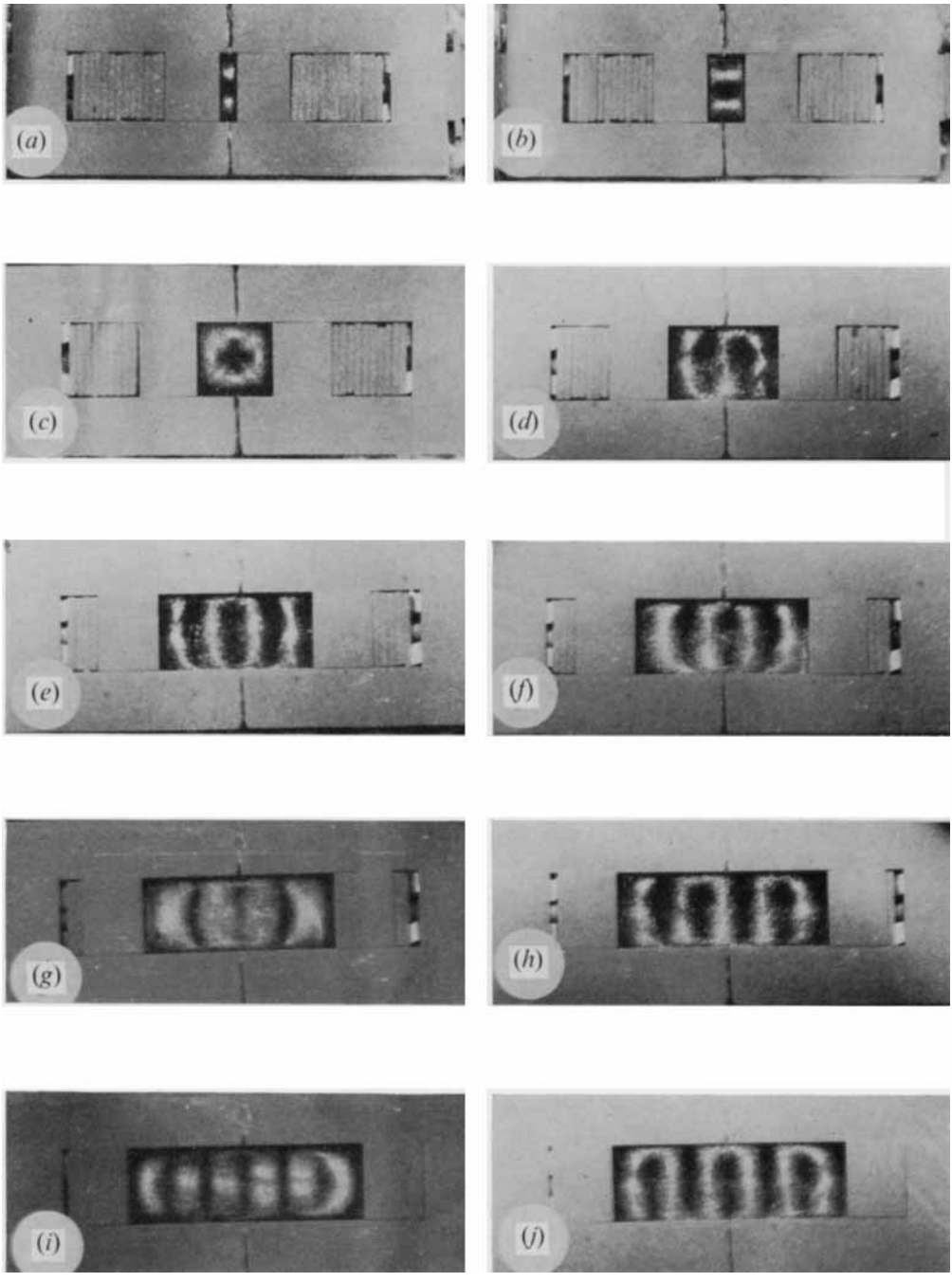


FIGURE 6. Convection cells in rectangular boxes with $h_1 = 4{\cdot}0$. (*a*) $h_2 = 0{\cdot}5$, 5 finite $x$-rolls. (*b*) $h_2 = 0{\cdot}9$, 4 finite $x$-rolls. (*c*) $h_2 = 1{\cdot}3$, 4 finite $x$-rolls. (*d*) $h_2 = 1{\cdot}9$, 4 finite $x$-rolls. (*e*), (*f*) $h_2 = 3{\cdot}5$, 2 different cell arrangements: symmetrical arrangement and 4 finite $x$-rolls. (*g*) $h_2 = 4{\cdot}0$, combination of $x$- and $y$-rolls. (*h*) $h_2 = 4{\cdot}3$, 4 finite $y$-rolls. (*i*) $h_2 = 5{\cdot}3$, 5 finite $y$-rolls. (*j*) $h_2 = 6{\cdot}0$, 6 finite $y$-rolls.

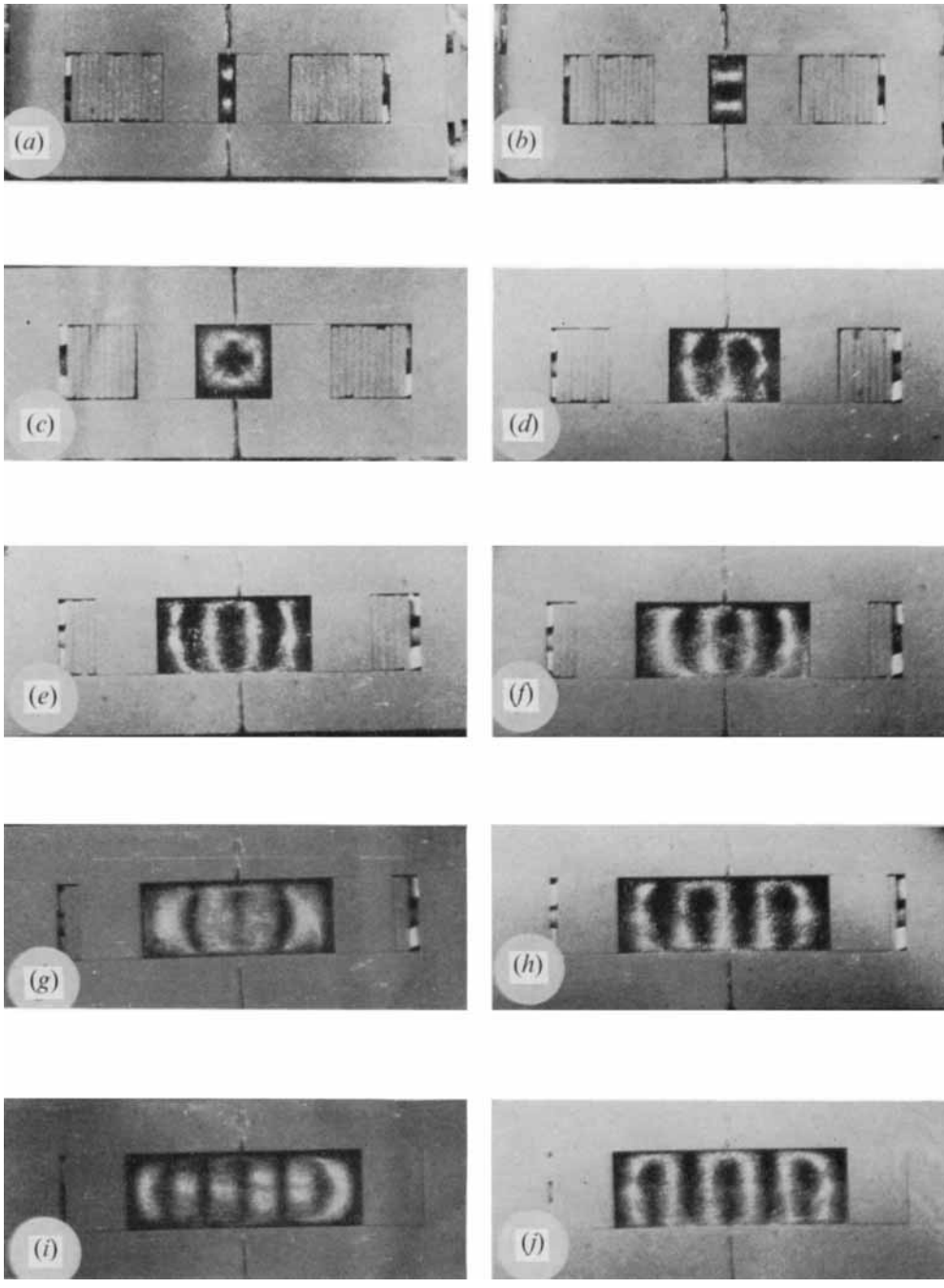


FIGURE 7. Convection cells in rectangular boxes with $h_1 = 5{\cdot}0$. (*a*) $h_2 = 0{\cdot}9$, 5 finite $x$-rolls. (*b*) $h_2 = 1{\cdot}5$, 5 finite $x$-rolls. (*c*) $h_2 = 1{\cdot}9$, 5 finite $x$-rolls. (*d*) $h_2 = 2{\cdot}7$, 5 finite $x$-rolls. (*e*) $h_2 = 3{\cdot}7$, 5 finite $x$-rolls. (*f*) $h_2 = 4{\cdot}7$, symmetrical arrangements of convection cells. (*g*) $h_2 = 5{\cdot}1$, symmetrical arrangements of convection cells. (*h*) $h_2 = 5{\cdot}5$, 5 $y$-rolls with small disturbances. (*i*) $h_2 = 5{\cdot}7$, 5 finite $y$-rolls. (*j*) $h_2 = 5{\cdot}9$, 6 finite $y$-rolls.

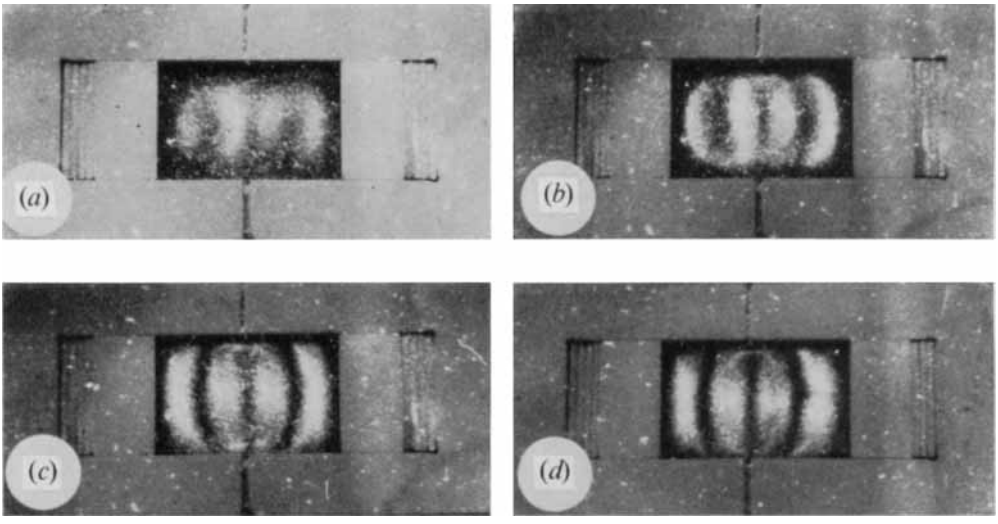


FIGURE 8. Four $y$-rolls at different stages of development in a box with $h_1 = 3{\cdot}0$, $h_2 = 4{\cdot}5$. ($a$) Onset of convection at the critical Rayleigh number. ($b$) Formation of the rolls 5 min after ($a$). ($c$) Formation of the rolls 10 min after ($a$). ($d$) Formation of the rolls 15 min after ($a$).

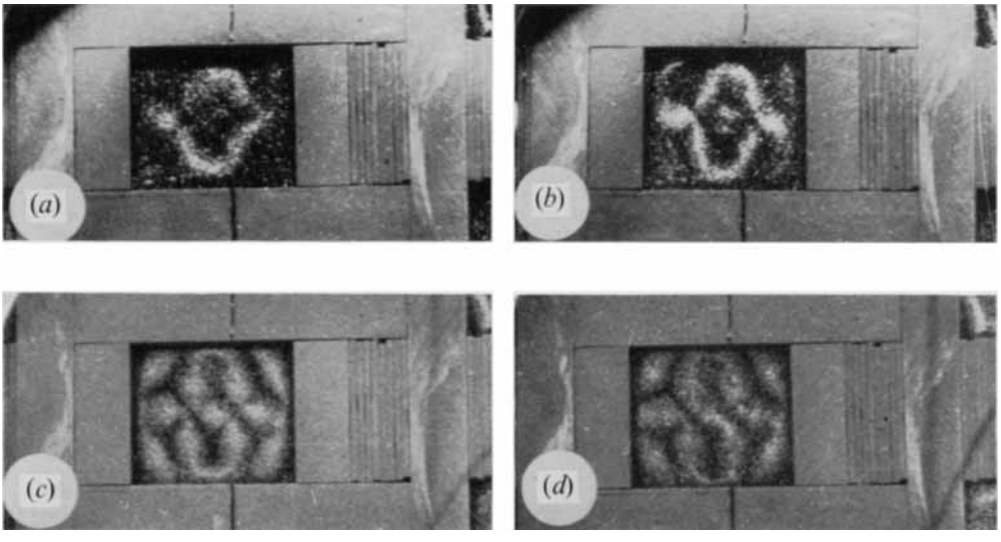


FIGURE 9. Symmetrical arrangement of convection cells at different stages of development in a box with $h_1 = 4{\cdot}0$, $h_2 = 4.5$. ($a$) Onset of convection at the critical Rayleigh number. ($b$) Formation 5 min after ($a$). ($c$) Formation 10 min after ($a$). ($d$) Formation 15 min after ($a$).

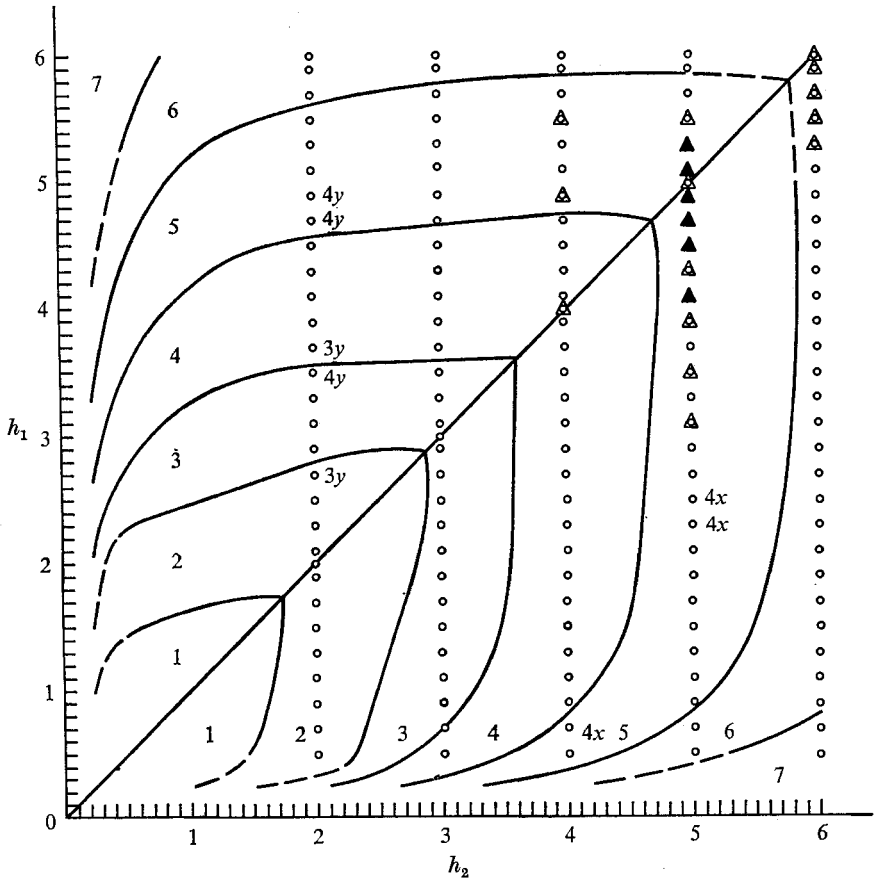


FIGURE 10. Map of preferred wavenumber (given by numbers between the solid lines) of finite rolls as a function of $h_1$ and $h_2$. The figure is symmetric with respect to the line $h_1 = h_2$. Finite $x$-rolls are preferred below the line $h_1 = h_2$ and finite $y$-rolls above. Characteristics of experimental results: ○, agreement between theory and experiments; ○3$y$, three finite $y$-rolls form, agreement in cell shape, no agreement in the number of cells; △, experimental results are comparable with the theoretical results but disturbances of the cell shape occurred; ▲, no agreement between experiments and theory (see § 3).

will not induce a decay into the more stable state as predicted by theoretical results.

*Test series* 2 ($h_1 = 3$). Theoretical and experimental results agree completely (see figure 10).

*Test series* 3 ($h_1 = 4$). The experiments with $h_2 = 4{\cdot}9$ and $h_2 = 5{\cdot}5$ exhibit irregularities. According to the theory five cells are to be expected. However, as the next series will show more clearly, the odd cell number five occupies a special position. Another discrepancy was realized in the marginal area of 4 and 5 possible rolls, where $h_1 < 1$. Accordingly, the explanation given above for test series 1 holds in this case (see figure 6).

*Test series* 4 ($h_1 = 5$). It can be seen from figure 10 that for $h_2 \geqslant 3$ in the majority of cases the five rolls expected did not appear. Rather, the following phenomena were observed. Symmetrically shaped cell arrangements formed (see

figure 7 (*f*)), rolls developed parallel to the diagonal of the rectangular frame (see figure 7 (*g*)), or slightly inclined rolls formed so that one of the rolls may only be partly developed (see figure 7 (*h*)). The question therefore arises as to how this unexpected phenomenon can be explained. When performing the experiments it was generally observed that at first an even number of rolls parallel to the shorter side wall or other symmetric arrangements formed. Only after some time did another roll develop under the influence of the side walls or did the symmetric patterns orient themselves to finite rolls. This could be observed also in test series 2, in which systems of three as well as of five finite rolls were observed. In test series 4, however, the influence of the side walls is considerably smaller than in test series 2, meaning that a transformation from a symmetric pattern to finite rolls is prevented by disturbances of stronger influence than the side walls. It should be noted that the variations of the liquid properties with temperature can be of considerable influence. Segel (1969) has pointed out in his article (see his figure 4) that such variations are expected to dominate the lateral wall effects for large aspect ratios when roll-like or even polygonal cell shapes are preferred. Another important disturbance might be caused in the following way. In case of an odd number of finite rolls the number of upward- and downward-directed flow areas is odd. In particular, there is upward flow near the one of the two side walls which is parallel to the finite rolls and downward flow near the other. When the walls are not perfect heat conductors, temperature differences between the side walls may induce horizontal temperature gradients and affect convection flow to a large extent. It is known (see Koschmieder 1966; Müller 1966) that cellular convection can be strongly influenced by convection flow circulating over long distances.

*Test series* 5 ($h_1 = 6$). The experiments give an even number of finite rolls (see figure 10) according to theory. If the frame forming the side wall is of nearly square shape irregularities appear because the influence caused by the different lengths of the side walls is too small. Here we hint at another phenomenon which appeared generally in all experiments. The axis of the finite rolls near the side walls was bent towards the interior of the test volume; this means that the corners exert a strong influence. This phenomenon is not described by Davis' (1967) theory. It can be explained partly by the fact that finite rolls are not exact solutions of the linear problem (see Davies-Jones 1971) and partly by the imprecise thermal boundary conditions.

## 6. Concluding remarks

The most evident result of these experiments is the dependency of the critical Rayleigh number on the horizontal extension of the boxes. As the horizontal dimensions increase this number approaches rapidly the value of 1708, at which the onset of convection starts in thin horizontal layers heated from below. The second result is the proof that finite convection rolls form parallel to the shorter side wall of the box in the majority of cases. The numbers of finite rolls were in general such multiples of the layer heights that rolls of nearly squared cross-sections appeared. Only in case of very narrow boxes with $h_1 < 1$, where the

depth is not the smallest dimension, did rolls of cross-sections smaller than a square form. The reason is that the more restrictive no-slip condition increases the viscous dissipation. Therefore more potential energy must be released by the upthrust of the particles to sustain the convection, and this is achieved by the formation of narrower cells. When the boxes were of square or nearly square shape, i.e. $h_1 \approx h_2$, symmetric convection patterns were observed whose development can be considered as a state of equilibrium between rolls tending to align parallel to different side walls.

All the above observations are in good agreement with the theoretical results of Davis (1967). Discrepancies can be explained largely by taking into consideration the results of Davies-Jones (1971) for insulating rather than perfect heat-conducting boundaries. However, no theoretical results are known which might explain satisfactorily the phenomenon that the formation of an even number of finite rolls was preferred to the development of an odd number. As was reported in § 5.2, this phenomenon could be observed in several cases (see figure 10). However, it is felt that more detailed experimental and theoretical investigations of this behaviour are necessary before the phenomenon can be adequately explained.

The authors thank Mr U. Remde for his help during the performance of the experiments. The financial support of the Deutsche Forschungsgemeinschaft is gratefully acknowledged. This work was completed during a visit by one of the authors (U.M.) to the University of Queensland; the visit was made possible by a Postdoctoral Fellowship and the hospitality of the Department of Mechanical Engineering of that university.

## REFERENCES

CATTON, I. 1970 *Trans. A.S.M.E., J. Heat Transfer*, C **92**, 186.
CARSLAW, H. S. & JAEGER, J. C. 1959 *Conduction of Heat in Solids.*
DAVIES-JONES, R. P. 1971 *J. Fluid Mech.* **44**, 695.
DAVIS, S. H. 1967 *J. Fluid Mech.* **30**, 465.
JOSEPH, D. D. 1965 *Arch. Ration. Mech. Anal.* **20**, 59.
KOSCHMIEDER, E. L. 1966 *Beitr. Phys. Atmos.* **39**, 208.
MÜLLER, U. 1966 *Beitr. Phys. Atmos.* **39**, 217.
PELLEW, A. & SOUTHWELL, R. V. 1940 *Proc. Roy. Soc.* A **176**, 312.
SEGEL, L. A. 1969 *J. Fluid Mech.* **38**, 203.
ZIEREP, J. 1963 *Beitr. Phys. Atmos.* **36**, 70.